AMERICAN SOCIETY FOR MICROBIOLOGY | Applied and Environmental Microbiology®

Dietary Fatty Acids Sustain the Growth of the Human Gut Microbiota

Richard Agans,[a] Alex Gordon,[a] Denise Lynette Kramer,[a] Sergio Perez-Burillo,[b] José A. Rufián-Henares,[b] Oleg Paliy[a]

[a]Department of Biochemistry and Molecular Biology, Boonshoft School of Medicine, Wright State University, Dayton, Ohio, USA

[b]Department of Nutrition and Food Science, School of Pharmacy, University of Granada, Granada, Spain

ABSTRACT While a substantial amount of dietary fats escape absorption in the human small intestine and reach the colon, the ability of resident microbiota to utilize these dietary fats for growth has not been investigated in detail. In this study, we used an *in vitro* multivessel simulator system of the human colon to reveal that the human gut microbiota is able to utilize typically consumed dietary fatty acids to sustain growth. Gut microbiota adapted quickly to a macronutrient switch from a balanced Western diet-type medium to its variant lacking carbohydrates and proteins. We defined specific genera that increased in their abundances on the fats-only medium, including *Alistipes*, *Bilophila*, and several genera of the class *Gammaproteobacteria*. In contrast, the abundances of well-known glycan and protein degraders, including *Bacteroides*, *Clostridium*, and *Roseburia* spp., were reduced under such conditions. The predicted prevalences of microbial genes coding for fatty acid degradation enzymes and anaerobic respiratory reductases were significantly increased in the fats-only environment, whereas the abundance of glycan degradation genes was diminished. These changes also resulted in lower microbial production of short-chain fatty acids and antioxidants. Our findings provide justification for the previously observed alterations in gut microbiota observed in human and animal studies of high-fat diets.

IMPORTANCE Increased intake of fats in many developed countries has raised awareness of potentially harmful and beneficial effects of high fat consumption on human health. Some dietary fats escape digestion in the small intestine and reach the colon where they can be metabolized by gut microbiota. We show that human gut microbes are able to maintain a complex community when supplied with dietary fatty acids as the only nutrient and carbon sources. Such fatty acid-based growth leads to lower production of short-chain fatty acids and antioxidants by community members, which potentially have negative health consequences on the host.

KEYWORDS Western diet, dietary fats, microbial digestion, microbiota, nutrition

The human diet not only supplies vital nutrients, but it also influences life span (1) and the physiological state of many organs, as well as contributes to the development of diseases, such as obesity, type 2 diabetes (T2D), cardiovascular and inflammatory diseases, and several cancers (2). The prevalence of nutrition-related disorders has increased in recent decades to a state where one-third of the U.S. population can be classified as suffering from metabolic syndrome (3).

Many dietary effects on human health are mediated by the function of gut microbes. This is because a significant proportion of ingested foods escapes digestion and absorption in the small intestine and reaches the colon, a section of the gut housing a dense population of microbes. These compounds include dietary fiber, resistant starch,

Received 20 June 2018 **Accepted** 27 August 2018

Accepted manuscript posted online 21 September 2018

Citation Agans R, Gordon A, Kramer DL, Perez-Burillo S, Rufián-Henares JA, Paliy O. 2018. Dietary fatty acids sustain the growth of the human gut microbiota. Appl Environ Microbiol 84:e01525-18. https://doi.org/10.1128/AEM.01525-18.

Editor Edward G. Dudley, The Pennsylvania State University

Address correspondence to Oleg Paliy, oleg.paliy@wright.edu.

small amounts of simple carbohydrates, dietary proteins, and fats, as well as bile salts and enzymes released in the small intestine (4, 5). Most of these unabsorbed compounds are fermented in the colon by the gut microbiota. For example, intestinal microbes degrade undigested polysaccharides via anaerobic fermentation to various short-chain fatty acids (SCFAs), such as butyrate, propionate, and acetate. These SCFAs are then readily absorbed and used by the colonic enterocytes as well as by cells of other tissues as a source of energy and carbon (6). Whereas end products of carbohydrate fermentation serve positive functions in the gut, protein digestion has been shown to be detrimental to the host health due to the accumulation of harmful phenolic compounds, ammonia, and hydrogen disulfide in the colon (5, 7). The consumption of large quantities of meat is associated with an increased risk of developing colon cancer (8), which is possibly associated with an elevated production of the above-mentioned harmful compounds by intestinal microbiota (9).

Much less is known about microbial degradation of dietary fats in the human gut, possibly because it was assumed that these compounds were absorbed in the small intestine (10). However, combining the data from several reports that measured the amounts of fatty acids in the colon as well as the absorption of different fatty acids in the small intestine (11–13), it is clear that a portion of ingested fats enters the human colon each day. Increased consumption of dietary fats on a Western diet likely saturates the ability of small intestine to emulsify and absorb all dietary lipids, thus allowing a considerable fraction to avoid absorption and reach the colon (14). This conclusion is supported by multiple studies which showed that a high-fat diet leads to significant alterations in gut microbial communities in both humans and animals (15, 16). For example, in mice, a high-fat diet resulted in decreased *Bifidobacterium* content, which correlated with higher plasma lipopolysaccharide levels, thereby allowing the onset of inflammation, insulin resistance, and T2D associated with obesity (17). In another study, high-fat-diet feeding of mice correlated negatively with *Akkermansia* abundance but positively with the levels of *Bilophila* (18). In addition, a diet high in animal fat stimulated the growth of secondary bile acid-producing bacteria (19), and studies have shown that secondary bile acids are cytotoxic and carcinogenic.

Despite the recognition of the detrimental gut microbiota-mediated effects of a high-fat diet on human health (20), there is a significant gap in our understanding of which microbiota members are primarily responsible for lipid degradation and what the specific consequences of high-dietary-fat consumption on microbiota structure and functions are. To a large extent, the lack of such information can be related to the extreme difficulty of providing fat-exclusive diets to human volunteers and to rodent animal models as well. To fill these gaps, we built and validated a multivessel *in vitro* human gut simulator (HGS) system and then used that system to assess the ability of the human gut microbiota to utilize dietary fats for colonization and growth.

RESULTS

Design and validation of an *in vitro* human gut simulator. We built a three-vessel simulator system of the human gut by extending the previously published models (21, 22). The design of the system is shown in Fig. 1A. Each vessel of the HGS was seeded with an identical aliquot of fecal microbiota obtained from healthy adult donors. The HGS was validated to maintain anaerobicity, closed state (no contamination of the sterile medium in the assembled system with any environmental microbes), and precise temperature, pH, and transfer rate over a test period of 4 weeks. Figure 1B shows that the community in each vessel stabilized within the first 8 to 12 days of cultivation and community composition and then remained stable over several weeks of observation, similar to the findings from previous reports (23). The established communities resembled the original fecal inocula in comparison with unrelated human fecal sample (statistically significant similarity observed [Fig. 1C]). Not surprisingly, the similarity to fecal microbiota was highest for the distal vessel community. The microbes stratified among the vessels in agreement with the expected gradients of microbial concentrations along the colon (24). To illustrate this point, Fig. 1D shows that the levels of

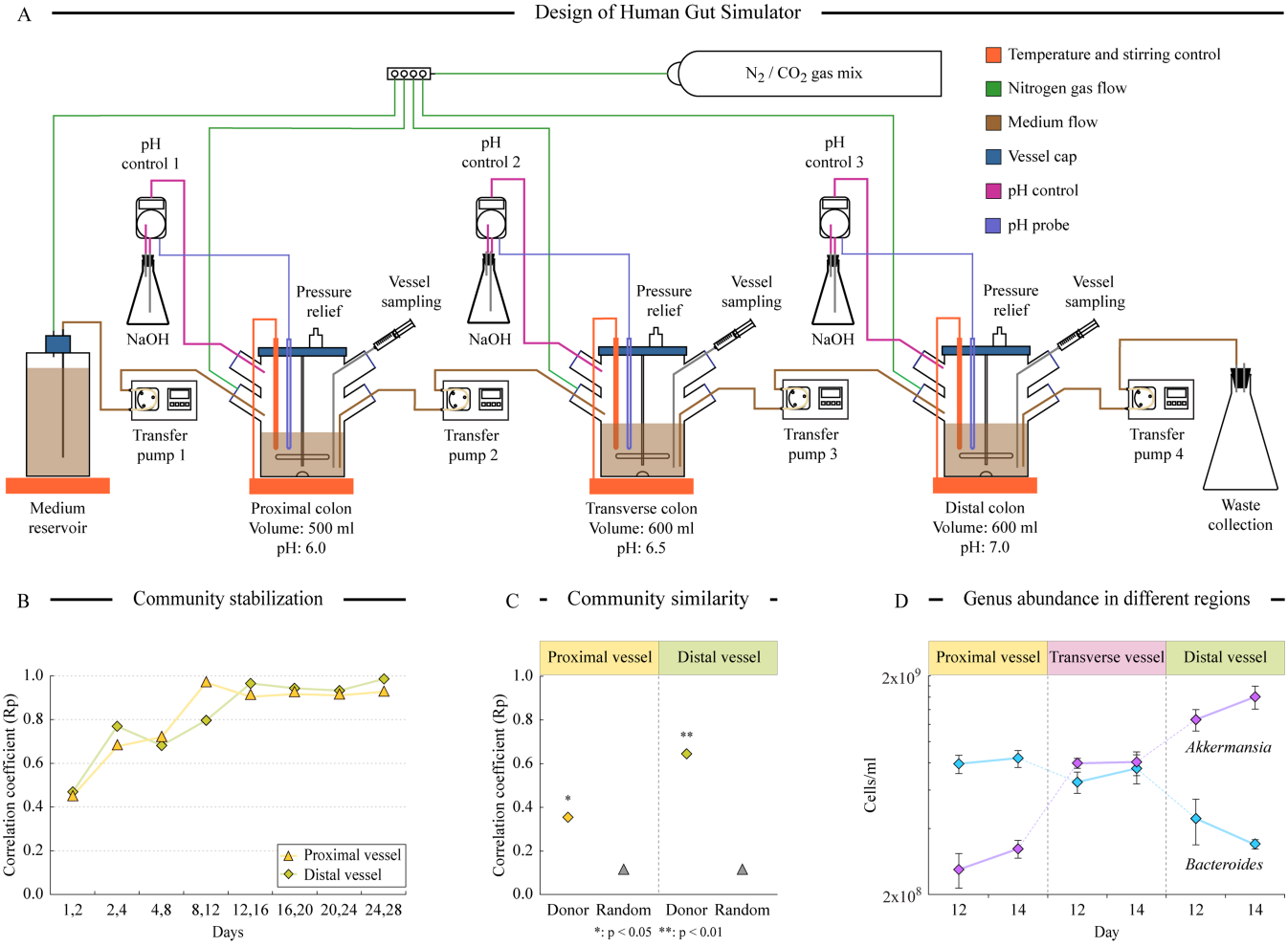

FIG 1 Design of human gut simulator (HGS) and validation of its performance. (A) Schematic representation of HGS design. (B) Results of the TRFLP analysis of community genomic DNA isolated from proximal and distal vessels on different days after the initialization of the system. Each point represents a Pearson correlation coefficient (R_p) between TRFLP profiles of two consecutive time points. (C) Similarities (R_p values) of HGS community (day 28) to those of the donor fecal sample and fecal sample from a random human volunteer. (D) Abundances of two prominent human gut microbiota genera in different vessels. Note that cell density is shown on a $\log_{10}$ scale (*y* axis). Error bars represent standard deviation of measurements between two runs.

polysaccharide- and protein-degrading *Bacteroides* spp. decreased from the proximal to distal vessel, in concordance with the gradient of dietary glycan and protein availability. Mucin-degrading *Akkermansia* spp. displayed the opposite trend due to its ability to degrade host mucins that were added in equal amounts to each vessel (Fig. 1D).

Microbial community response to removal of carbohydrates and proteins. To assess the ability of the human gut microbiota to utilize dietary fatty acids as the only readily available source of carbon and energy, we first established a stable community in each HGS vessel on a balanced medium that resembled colon influent on a typical Western diet. This Western medium (WM) contained complex and simple saccharides, proteins, and fats in proportions matching previously reported amounts in the human colon (Table 1) (13, 22). After 14 days of stabilization, the WM was switched to a fats-only variant, where all carbohydrates and proteins were removed, with the exception of a small amount of yeast extract that was a necessary source of vitamins and cofactors but which also contains carbohydrates and amino acids. Mucins were also removed from all three vessels to prevent microbes from relying on these glycoproteins and thus confounding the determination of which community members can be sustained specifically by dietary fats. The microbiota of the proximal vessel responded to this change in the supplied medium within 24 h, as was evident from the sharp drop in the community cell density on day 15 (Fig. 2A). A similar initial decline in the

TABLE 1 Medium composition

Medium component (g/liter)	Medium[a]		
	WM	FOM	YEM
Carbohydrates			
Arabinogalactan	1.8		
Cellobiose	0.9		
Fructose	0.5		
Glucose	0.5		
Guar gum	0.9		
Inulin	0.9		
Pectin	1.8		
Starch	4.4		
Xylan	0.9		
Proteins			
Casein	2.0		
Peptone	3.3		
Lipids			
Capric acid ($C_{10:0}$)	0.3	0.3	
Palmitic acid ($C_{16:0}$)	1.5	1.5	
Stearic acid ($C_{18:0}$)	0.7	0.7	
Oleic acid ($C_{18:1}$)	1.8	1.8	
Linoleic acid ($C_{18:2}$)	1.2	1.2	
Mucin	4.0		
Yeast extract	3.0	3.0	3.0
Salts, other components	14.9	14.9	14.9
Bile salts	1.0	1.0	

[a]WM, Western medium; FOM, fats-only medium; YEM, yeast extract medium.

community cell density was also observed in the transverse and distal vessels, with an expected delay of response accounting for the transit time required for the new medium to reach the second and third vessels. Interestingly, the cell densities in all three vessels partially recovered after the initial drop. This recovery in cell density coincided with a decrease in the average size of cells and the lowering of cell metabolic activity in proximal vessel, as displayed in Fig. 2B and 3A, respectively. Note that while 146.6 $\pm$ 4.3 kcal $\cdot$ liter^{-1} of macronutrient based energy was available in the Western medium, fats-only medium (FOM) only contained 57.0 $\pm$ 0.6 kcal $\cdot$ liter^{-1} (39% of that of the WM), as determined by bomb calorimetry. The final stabilized cell density of communities grown in FOM was 56 to 57% of that observed on the Western medium (Table 2). Because FOM also contained yeast extract, an additional run was performed with the medium containing yeast extract and salts only (Table 1). Community density was drastically lower in all three vessels when supplied such yeast extract medium (Fig. 2A) and constituted only 5 to 7% of that on the WM (Table 2). Taken together, these data indicate a preference of the community to decrease cell size in order to maintain comparable cell density and division rate upon the switch to environments with lower nutrient availability. This possibly represents a solution to avoid cell washout from the colon when the supply of foods is reduced (25).

Since oxygen is displaced passively in the HGS system by N_2/CO_2 sparging, it is possible that residual oxygen can serve as the primary electron acceptor during fatty acid oxidation. To rule out that possibility, we performed batch-culture growth tests of HGS inocula in the anaerobic chamber system, where oxygen is completely removed (below 1 ppm) via a palladium-catalyzed reaction with H_2 gas. As displayed in Table 2, community densities in three different media in these anaerobic tests were similar to those measured in the HGS experiments. These experiments provided further evidence that human gut microbiota can utilize dietary fatty acids anaerobically for growth and community maintenance.

Changes in community composition in response to the shift to fats-only medium. We used high-throughput 16S rRNA gene amplicon sequencing to assess the

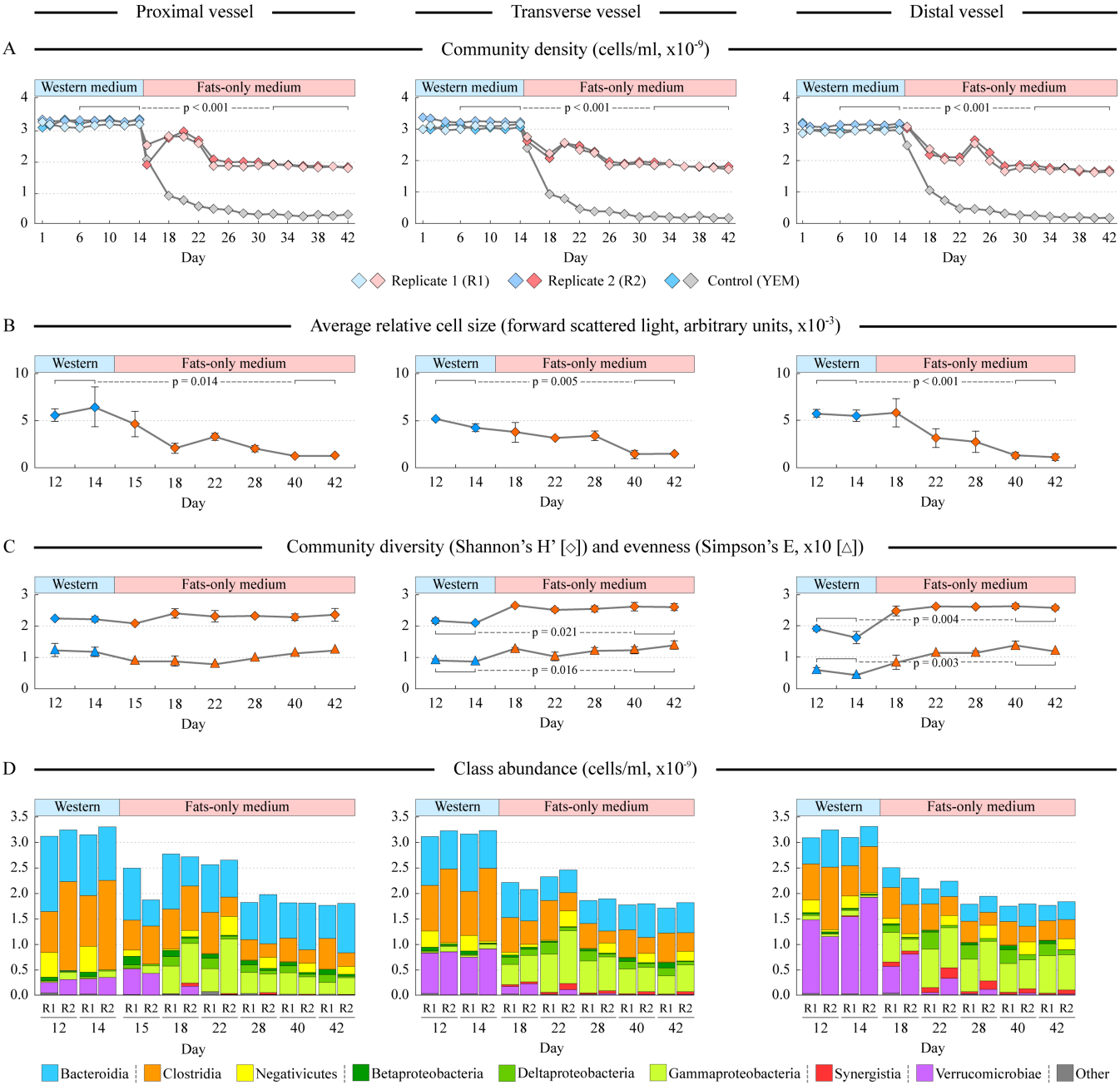

FIG 2 Dynamic changes in community density and composition during switch of the supplied medium. Different columns represent data for proximal, transverse, and distal vessels, as shown. The medium was switched from a medium resembling a balanced Western diet to fats-only medium after taking samples on day 14. In a control run, YEM containing only yeast extract and salts was used on days 15 to 42. (A) Cell density in each vessel. (B) Average relative cell size as measured by forward light scatter in flow cytometry analysis. (C) Calculations of genus-level based community diversity and evenness. Error bars in panels B and C represent standard deviations of measurements between two replicate runs. (D) Cumulative abundance of different bacterial classes at each time point. R1 and R2 represent individual replicate runs. Where shown, *P* values indicate statistically significant differences of the measured values between Western and fats-only media, as tested by repeated-measures ANOVA.

structure of microbial communities at each time point. To reduce biases in community composition estimates associated with the use of any single region of the 16S rRNA gene (26), we profiled both the V1–V2 and V4 16S rRNA gene regions. To reduce the PCR drift-associated bias of 16S rRNA gene amplification (27), 10 cycles of linear PCR were incorporated prior to exponential PCR phase. The distribution of diversity and evenness measures of community organization among vessels and between different media are shown in Fig. 2C. There was a noticeable gradient of decreasing community

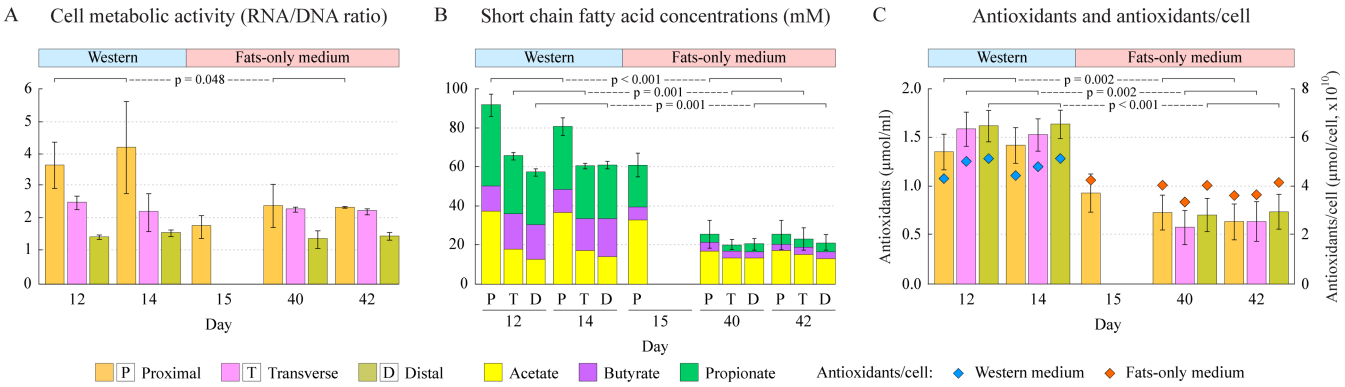

FIG 3 Metabolic profiling of HGS communities. (A) Average cell metabolic activity as measured by the ratio of total RNA to total DNA in cells. (B) Concentrations of the most abundant short-chain fatty acids. (C) Total antioxidant capacity (defined as equivalent to micromoles Trolox standard; shown on left-hand *y* axis) and antioxidant capacity per cell (shown on right-hand *y* axis) in different vessels. Error bars represent the standard deviation of measurements between two replicate runs; in panel B, only errors for the total amount of measured SCFAs are shown. Note that on day 15, samples were only taken from the proximal vessel because the change of the supplied medium would not have yet impacted the other two vessels. Statistically significant differences ($P < 0.05$, repeated-measures ANOVA) of the measured values between Western and fats-only media are indicated by connecting bars; *P* values in panel B indicate statistical significance of the total SCFA differences between conditions.

evenness and richness from the proximal to the transverse to the distal vessels ($P \leq 0.01$). This effect was largely attributed to a very high abundance of mucin-degrading *Akkermansia* spp. in the transverse and especially distal vessels. The high prevalence of this single genus is explained by the transverse and distal vessels containing an ample amount of mucins but not receiving any other nutrients directly (the medium is moved from proximal vessel after it has been subjected to the fermentation there). Removing *Akkermansia* members from the data set largely evened out the measures of richness (Shannon H′ index) and evenness (Simpson E index) among the vessels (data not shown). Upon the switch to the fats-only medium, the measures of the richness and evenness remained unchanged for the proximal vessel community, but they increased for the transverse and distal vessels (see Fig. 2C). This observed increase in community richness in the transverse and distal vessels was due to the more even distribution of cell counts among different phylogenetic clades in FOM, in large part because the lack of mucin previously supplied to these vessels led to a disappearance of highly abundant *Akkermansia* species.

The community composition on the balanced Western medium was predictably dominated by members of the classes *Clostridia* and *Bacteroidia*, with a significant presence of *Verrucomicrobiae* (mostly *Akkermansia* spp.) in transverse and distal vessels (Fig. 2D). The switch to FOM led to a significant reduction in the overall abundance of *Clostridia*, with a smaller decrease in *Bacteroidia* and almost complete disappearance of *Verrucomicrobiae*. In contrast, the numbers of different clades of *Proteobacteria* increased (see Fig. 2D).

These changes in community composition were significant enough to be the main source of variability in the genus abundance data set. Phylogenetic UniFrac distance-based principal-coordinate analysis (PCoA) separated samples largely according to the medium supplied at a particular time point (Fig. 4A). Interestingly, while the cell counts in the proximal vessel dropped noticeably 24 h after the medium switch (day 15 of the run; see Fig. 2A), the community composition had not had sufficient time to change, as was evident by the clustering of day 15 samples from the proximal vessel with day 12 and day 14 samples in the PCoA ordination plot (Fig. 4A). Constrained canonical ordination analysis (28) similarly revealed that the type of supplied medium was the dominant predictor of community composition, accounting for 47% of the overall data set variance (see Fig. 4B and C).

To quantitatively determine which specific genera drove the observed alterations in community structure, we performed a weighted UniFrac distance-based principal response curves (dbPRC) analysis (see reference 29) on our genus abundance data set.

TABLE 2 Steady-state cell densities

Culturing system	WM[a]	FOM[a]	% WM	YEM[a]	% WM
Human gut simulator					
Proximal vessel	3.21 ± 0.03	1.82 ± 0.01	56.6	0.22 ± 0.01	6.8
Transverse vessel	3.14 ± 0.04	1.77 ± 0.02	56.6	0.17 ± 0.01	5.3
Distal vessel	3.13 ± 0.04	1.76 ± 0.02	56.2	0.18 ± 0.01	5.9
Batch cultures in anaerobic chamber (72 h postinoculation)	2.74 ± 0.15	1.57 ± 0.04	57.3	0.36 ± 0.06	13.0

[a]Data are shown as arithmetic mean ± standard error of the mean (SEM) in cells × 10^{-9} · ml^{-1}.

PRC is a partial redundancy analysis which can isolate the variance explained by a chosen explanatory variable (medium switch/collection time point, in our case) (28). As shown in Fig. 4D, microbial communities in all three vessels responded to the medium switch by changing community structure, with good concordance in community alterations between replicate runs. Genus weights incorporated into the dbPRC model identified the genera that contributed the most to the community alterations. The genera that could least adapt to the sudden disappearance of carbohydrates, proteins, and mucins included well-known carbohydrate-degrading members of *Clostridium* XIVa, *Roseburia*, *Bacteroides*, and *Dorea*, as well as mucin-degrading *Akkermansia* spp. (Fig. 4E). This void in the community was quickly filled by representatives of *Alistipes* and *Bilophila* and by members of *Gammaproteobacteria* (e.g., *Escherichia*/*Shigella*, *Enterobacter*, and *Citrobacter* spp.). Figure 4F shows that the abundances of these taxa increased rapidly upon the switch to the fats-only medium, and they remained abundant until the end of the experimental run.

Production of short-chain fatty acids and antioxidants is severely diminished on fats-only medium. To determine how the switch to fats-only medium impacted the production of short-chain fatty acids by gut microbiota, we measured the levels of acetate, butyrate, and propionate with high-performance liquid chromatography (HPLC). In Western medium, acetate and propionate were the primary end products of fermentation (Fig. 3B). The large amount of propionate produced by the gut microbiota in WM was likely due to the fact that this fatty acid is formed during mucin degradation, consistent with the finding that mucin-degrading *Akkermansia* spp. release more propionate than acetate during fermentation (30, 31). Longer transit time also favors propionate formation (32). As shown in Fig. 3B, the overall production of SCFAs was reduced dramatically upon the removal of carbohydrates and proteins from the medium (86.2 ± 7.3 mM total SCFAs in proximal vessel supplied with WM and 25.5 ± 10.3 mM with FOM; $P < 0.01$). This constituted a 70% decrease in the overall SCFA production, compared with the 61% decrease in the total energy supplied by the FOM in comparison to WM, making SCFA production less efficient in FOM. The decrease in SCFA production in the proximal vessel was already evident 24 h after the medium switch, in that the total SCFA concentration on day 15 was 71% of that on day 12 and 14 (see Fig. 3B). By the end of the observation period, the production of acetate diminished the least (concentration on days 40 and 42 was on average 46% of that on days 12 and 14) but was more striking for butyrate and propionate (33% and 12% of the Western medium levels, respectively). The differential reduction in SCFA levels is likely explained by the fact that acetate is a direct end product of the β-oxidation of fatty acids.

Similarly, the total antioxidant capacity was significantly higher in the WM-cultured communities, even after adjusting for the lower cell densities of communities grown on FOM (Fig. 3C). This reduction also occurred within 24 h after the medium switch.

Dietary fats select for community members carrying fatty acid degradation genes. To determine the functional basis for the observed changes in gut microbiota structure upon medium swap to FOM, we sought to determine the predicted repertoire of functional metabolic genes in the communities before and after the medium switch. By comparing PICRUSt-based predictions of the functional capacities of each commu-

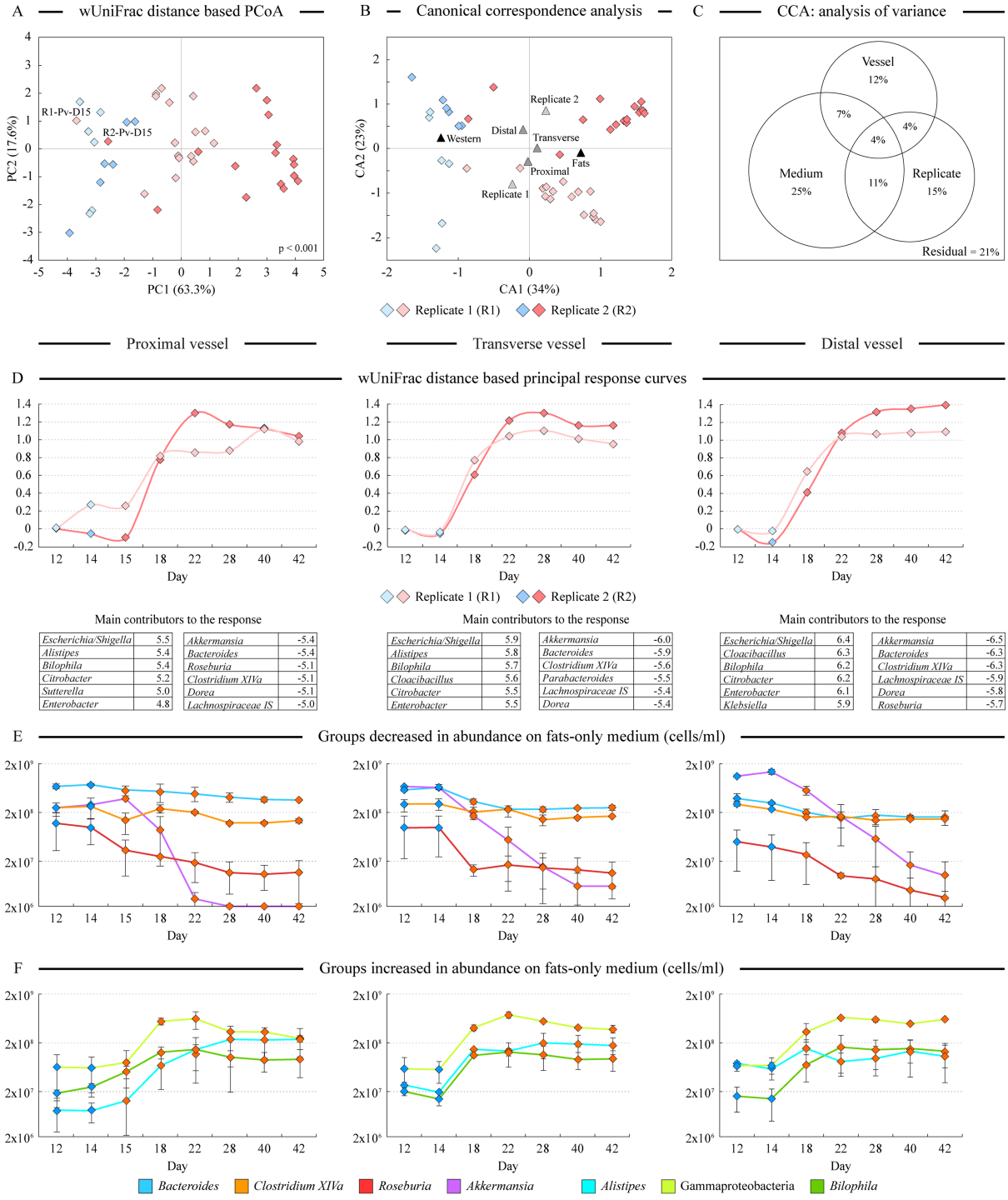

FIG 4 Analysis of community composition. (A) Output of the unconstrained principal-coordinate analysis (PCoA) of genus abundance data set among all profiled samples. Phylogenetic weighted UniFrac (wUniFrac) distance was used to calculate sample dissimilarity matrix. Blue points represent samples collected when supplying Western medium; red points represent samples collected after the switch to fats-only medium. Day 15 samples taken from the proximal vessel (Pv) are highlighted. *P* value denotes statistical significance of the separation of WM and FOM samples in PCoA space based on the permutation analysis of Davies-Bouldin index. (B) Output of the constrained canonical correspondence analysis (CCA). Medium type, vessel identity, and replicate run were used as explanatory variables that constrained the variability of the genus abundance data set. (C) The analysis of variance of the CCA output depicts the relative contributions of explanatory variables to the overall variability in the data set. (D) Results of weighted UniFrac distance-based principal response curves (PRC) analysis. Community composition at day 12 was set as the baseline and was compared to the composition at every other time point. Larger values on the *y* axis represent a greater shift in the community structure than that of day 12. The main drivers of the observed changes in the composition are shown in the tables. Positive numbers represent members that increased in their abundance after medium switch; genera with negative weights represent members that decreased the most in their abundance on fats-only medium. (E and F) The abundances of several of these genera at different time points. Note that cell density is shown on $\log_{10}$ scale (*y* axis). Error bars represent standard deviation of measurements between two runs.

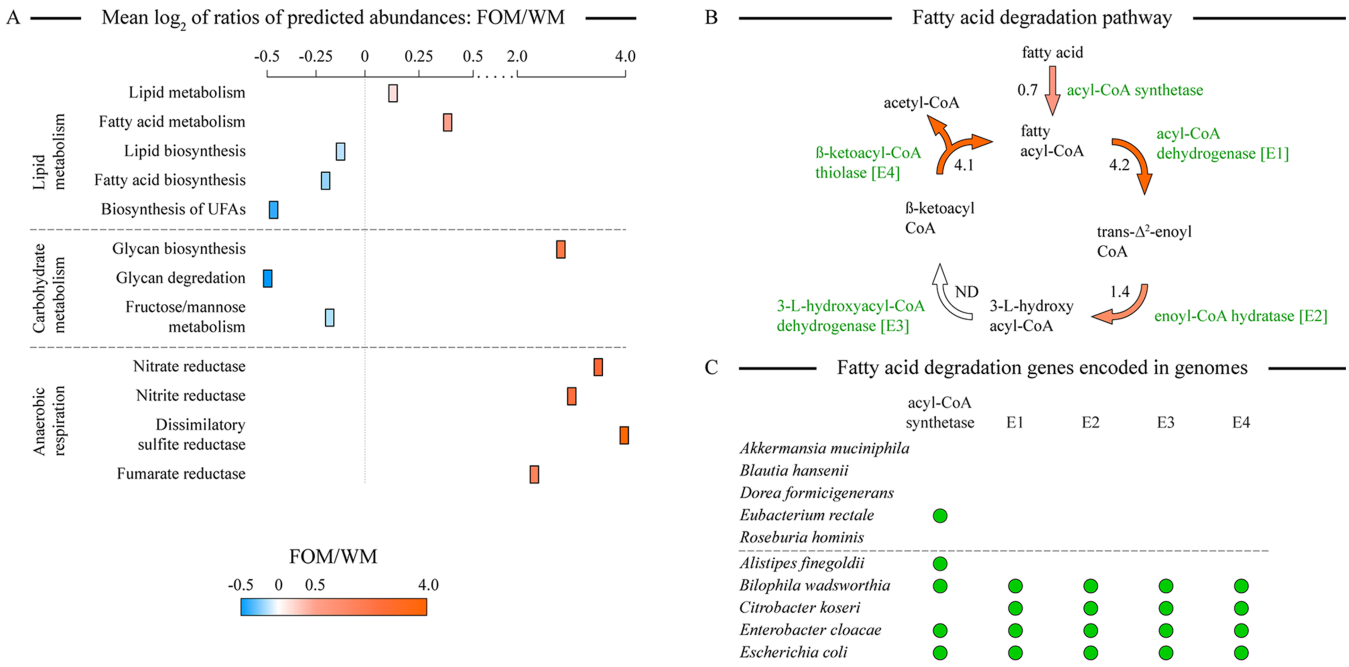

FIG 5 Analysis of predicted functional capacities of microbial communities. (A) Log_2-transformed ratios of predicted cumulative functional gene abundances for lipid and carbohydrate metabolism and anaerobic respiration between communities maintained on fats-only medium (FOM) and Western medium (WM). (B) Predicted log_2-transformed abundance ratios (FOM/WM) for the genes encoding the enzymes of fatty acid β-oxidation pathway. Arrows and rectangles are colored according to the abundance ratio color gradient, as shown in the legend. UFAs, unsaturated fatty acids; ND, not determined. (C) Predicted presence of β-oxidation pathway-encoding genes in genomes of microbes that either decreased (top) or increased (bottom) in abundance upon the WM-to-FOM switch. Gene presence prediction was based on KEGG and BioCyc genome annotations.

nity, we found that the overall abundance of the lipid degradation-related genes was higher in the communities maintained on the fats-only medium (see Fig. 5A). Looking at the fatty acid degradation pathway in-depth, we uncovered that the genes encoding the enzymes of the β-oxidation pathway were predicted to be substantially (between 1.6- and 18.4-fold) more prevalent in the FOM-adapted communities than in the microbiomes grown on the Western medium (Fig. 5B). At the same time, genes participating in the biosynthesis of fatty acids were less prevalent in FOM microbiomes, highlighting the presence of microbes accustomed to the availability of lipids in the environment. In contrast, the overall abundance of carbohydrate digestive enzymes was lower in these specialized communities, likely because many gut microbiota members with large repertoires of the carbohydrate-active enzymes (CAZymes) were not able to adapt to fat-exclusive nutrient supply and were outcompeted by fat-utilizing specialists. At the same time, the predicted abundance of glycan biosynthesis genes was higher on FOM, possibly because the members of that community are adapted to the low availability of carbohydrates in the environment and thus possess pathways to synthesize necessary glycans (e.g., cell wall components) from other compounds.

DISCUSSION

To carry out specific perturbation experiments of human gut microbiota, we have built and validated an *in vitro* multicompartmental human gut simulator system (see Fig. 1). The general features of this system are comparable to those of other *in vitro* gut simulators developed in several laboratories over the past 20 years (21, 22, 33–35). The two main advances of our design came from the redevelopment of the nutrient medium used in the HGS to include a mix of dietary fats calculated to match what reaches the colon daily, and in the careful programming of peristaltic pumps to control the frequency and order of medium transfer among compartments. The unique advantages of such *in vitro* gut systems compared to human and animal studies include

(i) the ability to disentangle the effects of diet on human gut microbiota from the effects of intestinal hormonal, electrolyte, and immune system responses; (ii) the ability to sample each section of the simulated "gut" frequently over long experimental time frames without ethical constraints or animal sacrifice; (iii) complete control of the environmental conditions, sampling, and nutrient changes, which give rise to highly robust results; and (iv) measurements of actual cell counts instead of relying on relative abundance values, which helps avoid assumptions and problems associated with the use of compositional (e.g., relative abundance) data. Point iv is important because the transformation of the data into relative form leads to a constant-sum constraint, which violates the assumption of variable independence in many statistical tests and can lead to spurious correlations (28). It is also important to recognize that such *in vitro* systems are not meant to mimic the human or animal intestine completely, because they lack intestinal epithelium with all of its components (immune cells, antimicrobial peptides, surface-bound mucus layer, nutrient absorption, electrolyte exchange, etc.). While the clinical relevance of simulator studies is thus lower than that in animal and clinical works, the *in vitro* gut simulators are well suited for analyses that focus on mechanisms of microbiota composition and function not directly affected by the host physiology (e.g., the effects of supplied nutrients in the diet).

The HGS system was used to carry out a 6-week-long temporal perturbation study that evaluated human gut microbiota utilization of dietary fats as the only readily available source of carbon and energy. Because such medium lacked almost all carbohydrates and proteins, this study would not be possible in human population or using common animal models. Surprisingly, the removal of carbohydrates and proteins did not lead to a drastic reduction in community cell density, as while the overall amount of energy in the environment decreased by 61%, cell density dropped only by 44%. The communities responded to the medium switch by reducing their cell size rather than numbers and by lowering their metabolic rate. Predictably, many gut microbiota members were not able to adapt to these conditions well, and we detected significant reductions in the abundances of both carbohydrate-utilizing (e.g., *Roseburia*, *Eubacterium*, and *Dorea* spp.) and protein-degrading (e.g., *Bacteroides* spp.) members (36). Among the genera that decreased the most on FOM, the vast majority did not possess any fatty acid oxidation enzymes, with the exception of few species encoding a putative acyl-coenzyme A (acyl-CoA) synthetase (Fig. 5C).

Several genera increased in abundance only once dietary fats remained in the medium, likely because they were able to utilize fats for growth and now had less competition for other nutrients. These "lipophilic" microbes included *Alistipes* spp. (class *Bacteroidia*) and many members of phylum *Proteobacteria*, including *Bilophila*, *Escherichia*/*Shigella*, *Citrobacter*, and *Enterobacter* species. The communities maintained on FOM were significantly enriched in the predicted abundances of fatty acid utilization genes, while at the same time, it was predicted that their genomes encoded far fewer carbohydrate utilization enzymes (see Fig. 5A). With the exception of *Alistipes* spp., the members of the lipophilic genera are predicted to possess the full complement of fatty acid degradation pathway genes and are thus capable of utilizing dietary fats for growth (see Fig. 5C). It is important to point out that not every microbe that maintained its presence in the FOM-grown communities is required to degrade dietary fats. It is likely that some members, such as *Alistipes* spp., relied on the metabolic cross-feeding of fermentation intermediates and end products released by the fat degraders (37, 38).

How can dietary fatty acids be utilized by human gut microbiota? The primary mechanism of deriving energy from free fatty acids is through the cyclic β-oxidation pathway, a ubiquitous pathway used by both eukaryotic (in mitochondria) and prokaryotic (in cytoplasm) organisms. Aerobically, acetyl-CoA formed during each cycle of fatty acid degradation can generate energy efficiently by entering the tricarboxylic acid cycle and passing electrons to an electron transport chain (39). However, under anaerobic conditions, molecular oxygen is not available to accept electrons from cytochrome oxidase, whereas cells still need to regenerate FAD and NAD^+ consumed in acyl-CoA dehydrogenase and 3-hydroxy-acyl-CoA dehydrogenase reactions of the

TABLE 3 Comparison of microbial and metabolite changes in HGS system upon switch to fats-only medium to the results from previous high-fat-diet intervention studies

Taxon/metabolite	HGS	Result (previous studies)[a]
Alistipes	Increased	Increased (15, 58–60)
Bilophila	Increased	Increased (58, 59, 61)
Proteobacteria	Increased	Increased (16, 60, 62)
Bacteroides	Decreased	Decreased (16, 62) Increased (58)
Clostridium	Decreased	Decreased (15, 61)
Eubacterium/Roseburia	Decreased	Decreased (15, 58)
Acetate	Decreased	Decreased (58, 59, 61) Increased (63)
Butyrate	Decreased	Decreased (58, 59, 61)
Propionate	Decreased	Decreased (59, 61)

[a]Comparison to published human and animal studies of high-fat diets.

β-oxidation pathway, respectively. This can be accomplished via anaerobic respiration with sulfate, nitrate, nitrite, or fumarate serving as terminal electron acceptors instead of oxygen (40). In line with the higher predicted prevalence of genes encoding fatty acid β-oxidation pathway enzymes in FOM microbiota, the FOM community genomes were also predicted to be enriched in the genes coding for anaerobic terminal reductases (Fig. 5A). The combination of β-oxidation and anaerobic respiration pathways would thus enable these bacteria to degrade free fatty acids and generate energy under anaerobic conditions.

Our findings provide mechanistic evidence for the increased prevalence of specific microbes in the guts of humans and animals fed a high-fat diet. Table 3 demonstrates a strong concordance of our HGS-based results with the outcomes from many previous high-fat-diet intervention studies. Specifically, the majority of those studies found that *Alistipes* spp., *Bilophila* spp., and total *Proteobacteria* increased on high-fat diets, and we observed that members of these taxa adapted well to the FOM (see Fig. 4F). In contrast, many high-fat-feeding reports, as well as our experiments, indicated reductions in *Bacteroides*, *Clostridium*, and *Eubacterium* spp. and several other genera of the class *Clostridia* on a high-fat diet. Finally, we showed that overall production of short-chain fatty acids is reduced on fats-only medium, also matching the majority of the findings from previous reports (Table 3).

The relative beneficial and harmful effects of the high-carbohydrate and high-fat diets are a subject of many studies and debates (41). While epidemiological studies show that an increase in dietary sugars and refined polysaccharides is associated with the higher prevalence of metabolic syndrome and type 2 diabetes (42), diets rich in fiber and complex polysaccharides promote SCFA production in the gut and provide a variety of beneficial effects. On the other hand, while dietary saturated fatty acids have been linked to increased serum low-density lipoprotein cholesterol (LDL-C), the LDL-C response is highly variable, and many studies do not support a direct link between dietary saturated fat and risk of heart disease (43). Indeed, several recent studies indicated that low-carbohydrate diets can elicit improvement in the diverse signs and symptoms of insulin resistance and its secondary manifestations, such as obesity and metabolic syndrome (44, 45). One aspect rarely considered in the above-mentioned debate is how macronutrient composition of a diet impacts the environment of the colon and the gut microbiota residing in that region. In this study, we showed that the human gut microbiota can utilize dietary fatty acids to sustain growth. Significant changes in community composition and predicted functional capacity occurred on such a fat-exclusive diet. Such changes led to a substantial decrease in the production of SCFAs and antioxidants in the colonic region of the gut, which might have negative health consequences on the host (46).

MATERIALS AND METHODS

Design of the gut simulator system. The design of a three-vessel *in vitro* human gut simulator (HGS) system was based on previously published models (21, 22) and is shown in Fig. 1. The HGS system consisted of three continuously linked fermentation vessels, each mimicking environmental conditions of the specific sections of the colon which house the majority of human gut microbes. Vessel 1 simulated the proximal colon, vessel 2 simulated the transverse colon, and vessel 3 modeled the distal colon (21, 47). The medium (Table 2), which closely matched food bolus contents that reach the colon (11, 21, 48), was supplied to vessel 1, and vessel contents were moved "along the colon" in 42-ml pulses every 2 h. The medium transfer rate was set to allow an overall system retention time of 72 h to mimic the experimentally derived upper estimate of the transit time within the human colon (49, 50). The vessel volumes were set to 500 ml, 600 ml, and 600 ml, respectively. Medium was transferred between vessels via FlexFlo peristaltic pumps (Cole Parmer, Inc.). The environmental conditions (temperature, pH, relative volume, and movement of contents) in each vessel matched those experimentally measured in the corresponding section of the human gut (4, 50, 51). Temperature (37°C) and agitation (60 rpm) were controlled via Isotemp hot stir plates (Thermo Scientific) equipped with in-vessel temperature probes (Omega Engineering). The pH was controlled automatically using Etatron pH pumps (Cole Parmer, Inc.) and reservoir of 0.5 M NaOH. An anaerobic atmosphere was maintained through periodic daily sparging of each vessel headspace with filtered O_2-free 90%–10% mix of N_2 and CO_2 gases. Fermentation vessels were equipped with syringe adaptors, which enabled direct sampling from each vessel. A concentrated mucin solution (made from porcine gastric mucin) was supplied via syringe injection equally to all three vessels at a rate of 2 g per day.

Preparation of fecal microbiota inocula. Fecal material was collected from three healthy male volunteers (27 to 31 years old) who had no history of antibiotic or probiotic use, and no gastrointestinal illness for 6 months immediately preceding the fecal collection. All fecal samples were mixed together and thoroughly homogenized to ensure that all inocula contained equivalent microbial populations. All fecal processing was performed on ice under N_2 atmosphere. Fecal slurries were prepared at 10% (wt/vol) in chilled anaerobic phosphate-buffered saline (PBS) and frozen.

Operation of human gut simulator. Two media were used to supply nutrients to microbial communities in the proximal vessel. The balanced Western medium was a rich medium containing carbohydrates, fats, and proteins in proportions matching the expected macronutrient distribution in colon influent on an average Western diet (55%, 20%, and 25%, respectively; see Table 2). The second medium (denoted fats-only medium [FOM]) was depleted in carbohydrates and proteins while maintaining the same level of dietary fatty acids (11%, 71%, and 18% of carbs, fats, and proteins, respectively). Resazurin was added to both media as an anaerobic indicator. All HGS vessels were seeded with a 50-ml aliquot of 10% fecal slurry and were incubated for 12 h to allow community establishment. The proximal vessel of the HGS system was then supplied semicontinuously (pulse every 2 h) with the Western medium (WM) for 14 days to allow community stabilization. At the end of day 14, the Western medium was replaced with the fats-only medium and the HGS system was operated for a further 28 days. Two completely independent 42-day-long runs were performed. In addition, a single control run was carried out where after 2 weeks on Western medium, the system was supplied with a medium containing only yeast extract and salts (denoted yeast extract medium [YEM]). To obtain cell density counts (in cells per milliliter) of each community, HGS samples collected from each vessel were diluted 100-fold, and cells were enumerated on Spencer hemacytometer via phase-contrast microscopy.

Anaerobic batch culturing. Ten-milliliter aliquots of WM, FOM, and YEM were first equilibrated for 24 h in an anaerobic atmosphere (85% N_2, 10% CO_2, and 5% H_2) inside the Coy anaerobic chamber. Cultures were then inoculated with fecal microbial inoculum identical to those used for HGS runs. All batch cultures were incubated inside the anaerobic chamber for 72 h to match the HGS transit time. Cell counting was performed as described above. Two replicate batch cultures were carried out for each type of medium.

Bomb calorimetry. A Parr 6200 isoperibol calorimeter (Parr Instrument Co.) was used to carry out isoperibol bomb calorimetry in order to determine the gross energy of growth media. Prepared aliquots of each medium were lyophilized, packed into capsules, weighed, and then combusted in the isoperibol bomb. Measurements were done in triplicate and calibrated to the energy of glycolic acid, and the capsule energy was subtracted from the total energy values obtained.

Isolation of nucleic acids and high-throughput DNA sequencing. Total nucleic acids were extracted following the hot phenol-chloroform method and incorporated a bead-beating step to break down microbial cells (27). Total RNA and DNA were quantified on Qubit 2.0 fluorometer using Qubit RNA BR and Promega Qubit double-stranded DNA (dsDNA) HS assay kits, respectively, according to the manufacturer's protocols. Community metabolic activity was defined as the ratio of total RNA to DNA based on previous studies showing an association between this measure and population metabolic activity (52, 53).

Bacterial genomic DNA was isolated from each HGS sample using the ZR fungal/bacterial DNA MiniPrep kit (Zymo Research), as we did previously (27). Genomic DNA (gDNA) was amplified using two pairs of primers, one targeting 16S rRNA gene V1–V2 region (forward primer 16S gene complementary sequence, AGRGTTYGATYMTGGCTCAG; reverse primer 16S gene complementary sequence, GCWGCCW CCCGTAGGWGT), and another targeting V4 region (forward [GCCAGCMGCCGCGG] and reverse [GGACT ACHVGGGTWTCTAAT] complementary sequences, respectively). Two different regions were interrogated to reduce biases in community composition estimates associated with the use of any one region of the 16S rRNA gene (26). Forward primers contained an Ion Torrent P1 adapter sequence, 6- to 7-nucleotide barcode sequence, and variable region-specific sequence. Reverse primer sequences included the

adapter A and variable region-specific sequence. PCR amplification was performed with 25 ng of starting gDNA material and included 10 cycles of linear elongation with only the forward primers used, followed by 25 cycles of traditional exponential PCR (54). The inclusion of a linear PCR step decreased the stochasticity of the first few PCR steps (27) and allowed the use of a single PCR amplification reaction per sample. Purified amplicons were pooled equimolarly, and sequencing libraries were prepared using the Ion PGM template OT2 400 kit (Life Technologies, Inc.), according to the manufacturer's protocol. High-throughput sequencing was performed on an Ion Torrent PGM using the Ion PGM sequencing 400 kit and Ion 316 Chip. We obtained an average of 40,129 sequence reads per sample. Sequence reads were processed in QIIME (55). For each sample, sequence reads for different 16S rRNA gene variable regions were subsampled to the lowest value and then merged. Annotation of operational taxonomic units (OTUs) was performed via an open reference method against the Ribosome Database Project reference database version 11 of 16S rRNA sequences. Any sequences with below 60% annotation confidence were labeled "unassigned" at that taxonomical level. To obtain cell counts, sequence read counts for each OTU were first adjusted by dividing them by a known or predicted number of 16S rRNA gene copies in that organism's genome, following a previously described approach (27). Incorporating 16S rRNA gene copy number information was shown previously to improve estimates of microbial diversity and abundance (56). For the OTUs annotated above the species level, an average of 16S rRNA gene copies in all organisms of the next taxonomical level (e.g., genus, and if no data for that genus, a family) was used to calculate an estimated 16S rRNA gene copy number. These 16S rRNA gene copy-adjusted read counts were then converted to sample-specific cell counts based on the previously determined cell density measurements for each sample. As a result, the sum of cells of all taxa within each sample equaled the cell density in that sample, so that a sample with higher cell density had a proportionally higher overall number of cell counts. This approach allowed us to estimate the actual cell counts for each taxon in every sample and not rely on the relative abundance values (28).

Terminal restriction fragment length polymorphism. Terminal restriction fragment length polymorphism (TRFLP) analysis was used to assess the stability of microbial communities during HGS validation experiments. Full-length 16S rRNA gene was amplified in a PCR, as described previously (27). Bact-27F and Univ-1492R primers were fluorescently labeled with 6-carboxyfluorescein (6-FAM) and 5-HEX fluorophores, respectively. Following amplification, three reaction mixtures were pooled and subjected to restriction endonuclease digestion by HaeIII and RsaI enzymes (New England BioLabs) at 37°C for 4 h. Restriction digests were prepared for genotyping by mixing 40 ng of digested sample with 8 μl of formamide. Samples were run on a 3730x capillary sequencer employing ROX500 internal standard for fragment size determination. Raw TRFLP profiles were annotated against the internal standards using the PeakScanner version 1.0 software and were further processed in Microsoft Excel utilizing custom-designed Visual Basic scripts. The scripts removed the ladder fragments and nonessential labels, reformatted character strings, and calculated sum of the peak areas/heights. Fragment peaks contributing less than 0.4% of the overall profile area were discarded.

Metabolite profiling. Collected samples were centrifuged and supernatants filtered to remove particles. Twenty microliters of each supernatant were injected onto an Aquasil C_{18} reverse-phase column attached to the HPLC system (Thermo Scientific). The mobile phase was 50 mM phosphate buffer and acetonitrile (99:1 ratio) at pH 2.8. Short-chain fatty acids were eluted at a flow rate of 1.25 ml $\cdot$ min^{-1} over a 30-min period and detected at a 210 nm wavelength. Standard curves were constructed for each acid over a range of 100 mM to 10 μM concentrations.

Antioxidant capacity in samples was estimated by measuring supernatant ability to neutralize and counteract oxidation by ABTS [2,2′-azino-bis(3-ethylbenzothiazoline-6-sulfonic acid)] radical. The supernatant was diluted 20-fold and mixed with a fresh 1:1 solution of 7 mM ABTS and 2.45 mM potassium persulfate. The reaction was measured colorimetrically at a 730 nm wavelength in triplicate. Trolox (6-hydroxy-2,5,7,8-tetramethylchroman-2-carboxylic acid) was used as a standard to create daily calibration curves for the ABTS-potassium persulfate solution. Antioxidant capacity was expressed as micromoles per milliliter of Trolox.

Bacterial cell size comparison. Bacterial cells were pelleted by centrifugation at 14,000 $\times$ *g* for 5 min. The supernatant was discarded, and the pellet was washed twice with 1 ml of isotonic Tris-buffered saline (TBS). The final pellet was diluted with TBS to an approximate cell concentration of 1 $\times$ 10^6 cells $\cdot$ ml^{-1} based on the cell density measurements of the cultures. Cells were then labeled with SYTO9 fluorescent dye and analyzed on an Accuri C6 flow cytometer, with 66 μl $\cdot$ min^{-1} flow rate, detection threshold of 1,000 relative fluorescence units, and 22-μm core size. The distribution of cell sizes was estimated from the forward-scatter values of all SYTO9-positive events.

Statistical analyses. Repeated-measures analysis of variance (ANOVA) was used to test the statistical significance of the differences in measured values between WM and FOM time points. Multivariate statistical analyses (principal-coordinate analysis, canonical correspondence analysis, and principal response curves) were performed on the genus-level microbial abundance data set generally following the approaches we described previously (28). Matlab- and R-based scripts were used to run all algorithms. Statistical significance of group separation in principal-coordinate analysis space was calculated based on the permutation analysis of the Davies-Bouldin index, as we did previously (57). Weighted UniFrac distance-based principal response curves (dbPRC) analysis was performed as described previously (29). This method used phylogenetic UniFrac distance as a measure of sample dissimilarity and carried out a partial redundancy analysis to isolate the part of the total data set variance attributable to sample collection time as a variable (see reference 28) for a more detailed explanation. dbPRC is especially suited to analyze time-series data sets (29).

Accession number(s). The sequence data set is available in the Sequence Read Archive repository under BioProject PRJNA487598.

ACKNOWLEDGMENTS

We are thankful to Vijay Shankar, Michael Bottomley, and Daniel Organisciak for valuable comments, and to Lynn Hartzler for access to a bomb calorimeter.

Parts of this work were supported by Dayton Area Graduate Studies Institute award RH15-WSU-15-1 to R.A., A.G., and O.P., by National Science Foundation award DBI-1335772 to O.P., and by award AGL2014-53895-R from the Spanish Ministry of Economy and Competitiveness and by the European Regional Development Fund (FEDER) to S.P.-B. and J.A.R.-H.

R.A. and O.P. conceived the study; R.A., A.G., D.L.K., and S.P.-B. carried out all experiments; and O.P., J.A.R.-H., and R.A. wrote the manuscript.

REFERENCES

1. Zhang C, Li S, Yang L, Huang P, Li W, Wang S, Zhao G, Zhang M, Pang X, Yan Z, Liu Y, Zhao L. 2013. Structural modulation of gut microbiota in life-long calorie-restricted mice. Nat Commun 4:2163. https://doi.org/10.1038/ncomms3163.
2. Van Horn LV. 2010. Report of the dietary guidelines advisory committee on the dietary guidelines for Americans. U.S. Department of Agriculture, Washington, DC.
3. Mozumdar A, Liguori G. 2011. Persistent increase of prevalence of metabolic syndrome among U.S. adults: NHANES III to NHANES 1999–2006. Diabetes Care 34:216–219. https://doi.org/10.2337/dc10-0879.
4. Cummings JH, Englyst HN. 1987. Fermentation in the human large intestine and the available substrates. Am J Clin Nutr 45:1243–1255. https://doi.org/10.1093/ajcn/45.5.1243.
5. Davis CD, Milner JA. 2009. Gastrointestinal microflora, food components and colon cancer prevention. J Nutr Biochem 20:743–752. https://doi.org/10.1016/j.jnutbio.2009.06.001.
6. Clausen MR, Mortensen PB. 1995. Kinetic studies on colonocyte metabolism of short-chain fatty acids and glucose in ulcerative colitis. Gut 37:684–689. https://doi.org/10.1136/gut.37.5.684.
7. Miyazaki K, Masuoka N, Kano M, Iizuka R. 2013. Bifidobacterium fermented milk and galacto-oligosaccharides lead to improved skin health by decreasing phenols production by gut microbiota. Benef Microbes 5:1–8. https://doi.org/10.3920/BM2012.0066.
8. Norat T, Lukanova A, Ferrari P, Riboli E. 2002. Meat consumption and colorectal cancer risk: dose-response meta-analysis of epidemiological studies. Int J Cancer 98:241–256. https://doi.org/10.1002/ijc.10126.
9. O'Keefe SJ, Ou J, Aufreiter S, O'Connor D, Sharma S, Sepulveda J, Fukuwatari T, Shibata K, Mawhinney T. 2009. Products of the colonic microbiota mediate the effects of diet on colon cancer risk. J Nutr 139:2044–2048. https://doi.org/10.3945/jn.109.104380.
10. Mu H, Hoy CE. 2004. The digestion of dietary triacylglycerols. Prog Lipid Res 43:105–133. https://doi.org/10.1016/S0163-7827(03)00050-X.
11. Jeppesen PB, Mortensen PB. 1998. The influence of a preserved colon on the absorption of medium chain fat in patients with small bowel resection. Gut 43:478–483. https://doi.org/10.1136/gut.43.4.478.
12. Kris-Etherton PM, Griel AE, Psota TL, Gebauer SK, Zhang J, Etherton TD. 2005. Dietary stearic acid and risk of cardiovascular disease: intake, sources, digestion, and absorption. Lipids 40:1193–1200. https://doi.org/10.1007/s11745-005-1485-y.
13. Kris-Etherton PM, Pearson TA, Wan Y, Hargrove RL, Moriarty K, Fishell V, Etherton TD. 1999. High-monounsaturated fatty acid diets lower both plasma cholesterol and triacylglycerol concentrations. Am J Clin Nutr 70:1009–1015. https://doi.org/10.1093/ajcn/70.6.1009.
14. Iqbal J, Hussain MM. 2009. Intestinal lipid absorption. Am J Physiol Endocrinol Metab 296:E1183–E1194. https://doi.org/10.1152/ajpendo.90899.2008.
15. Daniel H, Gholami AM, Berry D, Desmarchelier C, Hahne H, Loh G, Mondot S, Lepage P, Rothballer M, Walker A, Bohm C, Wenning M, Wagner M, Blaut M, Schmitt-Kopplin P, Kuster B, Haller D, Clavel T. 2014. High-fat diet alters gut microbiota physiology in mice. ISME J 8:295–308. https://doi.org/10.1038/ismej.2013.155.
16. Hildebrandt MA, Hoffman C, Sherrill-Mix SA, Keilbaugh SA, Hamady M, Chen YY, Knight R, Ahima RS, Bushman F, Wu GD. 2009. High-fat diet determines the composition of the murine gut microbiome independently of obesity. Gastroenterology 137:1716–1724. https://doi.org/10.1053/j.gastro.2009.08.042.
17. Cani PD, Neyrinck AM, Fava F, Knauf C, Burcelin RG, Tuohy KM, Gibson GR, Delzenne NM. 2007. Selective increases of bifidobacteria in gut microflora improve high-fat-diet-induced diabetes in mice through a mechanism associated with endotoxaemia. Diabetologia 50:2374–2383. https://doi.org/10.1007/s00125-007-0791-0.
18. Schneeberger M, Everard A, Gomez-Valades AG, Matamoros S, Ramirez S, Delzenne NM, Gomis R, Claret M, Cani PD. 2015. Akkermansia muciniphila inversely correlates with the onset of inflammation, altered adipose tissue metabolism and metabolic disorders during obesity in mice. Sci Rep 5:16643. https://doi.org/10.1038/srep16643.
19. Devkota S, Wang Y, Musch MW, Leone V, Fehlner-Peach H, Nadimpalli A, Antonopoulos DA, Jabri B, Chang EB. 2012. Dietary-fat-induced taurocholic acid promotes pathobiont expansion and colitis in IL10$^{-/-}$ mice. Nature 487:104–108. https://doi.org/10.1038/nature11225.
20. Shen W, Gaskins HR, McIntosh MK. 2013. Influence of dietary fat on intestinal microbes, inflammation, barrier function and metabolic outcomes. J Nutr Biochem 25:270–280. https://doi.org/10.1016/j.jnutbio.2013.09.009.
21. Gibson GR, Cummings JH, Macfarlane GT. 1988. Use of a three-stage continuous culture system to study the effect of mucin on dissimilatory sulfate reduction and methanogenesis by mixed populations of human gut bacteria. Appl Environ Microbiol 54:2750–2755.
22. Macfarlane GT, Macfarlane S, Gibson GR. 1998. Validation of a three-stage compound continuous culture system for investigating the effect of retention time on the ecology and metabolism of bacteria in the human colon. Microb Ecol 35:180–187. https://doi.org/10.1007/s002489900072.
23. McDonald JA, Schroeter K, Fuentes S, Heikamp-Dejong I, Khursigara CM, de Vos WM, Allen-Vercoe E. 2013. Evaluation of microbial community reproducibility, stability and composition in a human distal gut chemostat model. J Microbiol Methods 95:167–174. https://doi.org/10.1016/j.mimet.2013.08.008.
24. Peterson DA, Frank DN, Pace NR, Gordon JI. 2008. Metagenomic approaches for defining the pathogenesis of inflammatory bowel diseases. Cell Host Microbe 3:417–427. https://doi.org/10.1016/j.chom.2008.05.001.
25. Cremer J, Segota I, Yang CY, Arnoldini M, Sauls JT, Zhang Z, Gutierrez E, Groisman A, Hwa T. 2016. Effect of flow and peristaltic mixing on bacterial growth in a gut-like channel. Proc Natl Acad Sci U S A 113:11414–11419. https://doi.org/10.1073/pnas.1601306113.
26. Liu Z, DeSantis TZ, Andersen GL, Knight R. 2008. Accurate taxonomy assignments from 16S rRNA sequences produced by highly parallel pyrosequencers. Nucleic Acids Res 36:e120. https://doi.org/10.1093/nar/gkn491.
27. Rigsbee L, Agans R, Foy BD, Paliy O. 2011. Optimizing the analysis of human intestinal microbiota with phylogenetic microarray. FEMS Microbiol Ecol 75:332–342. https://doi.org/10.1111/j.1574-6941.2010.01009.x.
28. Paliy O, Shankar V. 2016. Application of multivariate statistical tech-

niques in microbial ecology. Mol Ecol 25:1032–1057. https://doi.org/10.1111/mec.13536.
29. Shankar V, Agans R, Paliy O. 2017. Advantages of phylogenetic distance based constrained ordination analyses for the examination of microbial communities. Sci Rep 7:6481. https://doi.org/10.1038/s41598-017-06693-z.
30. Derrien M, Vaughan EE, Plugge CM, de Vos WM. 2004. Akkermansia muciniphila gen. nov., sp. nov., a human intestinal mucin-degrading bacterium. Int J Syst Evol Microbiol 54:1469–1476. https://doi.org/10.1099/ijs.0.02873-0.
31. Lukovac S, Belzer C, Pellis L, Keijser BJ, de Vos WM, Montijn RC, Roeselers G. 2014. Differential modulation by Akkermansia muciniphila and Faecalibacterium prausnitzii of host peripheral lipid metabolism and histone acetylation in mouse gut organoids. mBio 5:e01438-14. https://doi.org/10.1128/mBio.01438-14.
32. Rios-Covian D, Salazar N, Gueimonde M, and de los Reyes-Gavilan CG. 2017. Shaping the metabolism of intestinal Bacteroides population through diet to improve human health. Front Microbiol 8:376. https://doi.org/10.3389/fmicb.2017.00376.
33. Kontula P, Jaskari J, Nollet L, De Smet I, von Wright A, Poutanen K, Mattila-Sandholm T. 1998. The colonization of a simulator of the human intestinal microbial ecosystem by a probiotic strain fed on a fermented oat bran product: effects on the gastrointestinal microbiota. Appl Microbiol Biotechnol 50:246–252. https://doi.org/10.1007/s002530051284.
34. Minekus M, Smeets-Peeters M, Bernalier A, Marol-Bonnin S, Havenaar R, Marteau P, Alric M, Fonty G, Huis in't Veld JH. 1999. A computer-controlled system to simulate conditions of the large intestine with peristaltic mixing, water absorption and absorption of fermentation products. Appl Microbiol Biotechnol 53:108–114. https://doi.org/10.1007/s002530051622.
35. Molly K, Vande Woestyne M, Verstraete W. 1993. Development of a 5-step multi-chamber reactor as a simulation of the human intestinal microbial ecosystem. Appl Microbiol Biotechnol 39:254–258. https://doi.org/10.1007/BF00228615.
36. Macfarlane GT, Cummings JH, Allison C. 1986. Protein degradation by human intestinal bacteria. J Gen Microbiol 132:1647–1656.
37. De Vuyst L, Leroy F. 2011. Cross-feeding between bifidobacteria and butyrate-producing colon bacteria explains bifidobacterial competitiveness, butyrate production, and gas production. Int J Food Microbiol 149:73–80. https://doi.org/10.1016/j.ijfoodmicro.2011.03.003.
38. Rakoff-Nahoum S, Coyne MJ, Comstock LE. 2014. An ecological network of polysaccharide utilization among human intestinal symbionts. Curr Biol 24:40–49. https://doi.org/10.1016/j.cub.2013.10.077.
39. Ingledew WJ, Poole RK. 1984. The respiratory chains of Escherichia coli. Microbiol Rev 48:222–271.
40. Campbell JW, Morgan-Kiss RM, and Cronan JE, Jr. 2003. A new Escherichia coli metabolic competency: growth on fatty acids by a novel anaerobic beta-oxidation pathway. Mol Microbiol 47:793–805. https://doi.org/10.1046/j.1365-2958.2003.03341.x.
41. Hu T, Mills KT, Yao L, Demanelis K, Eloustaz M, Yancy WS, Jr, Kelly TN, He J, Bazzano LA. 2012. Effects of low-carbohydrate diets versus low-fat diets on metabolic risk factors: a meta-analysis of randomized controlled clinical trials. Am J Epidemiol 176(Suppl 7):S44–S54. https://doi.org/10.1093/aje/kws264.
42. Morgantini C, Xiao C, Dash S, Lewis GF. 2014. Dietary carbohydrates and intestinal lipoprotein production. Curr Opin Clin Nutr Metab Care 17:355–359. https://doi.org/10.1097/MCO.0000000000000059.
43. Skeaff CM, Miller J. 2009. Dietary fat and coronary heart disease: summary of evidence from prospective cohort and randomised controlled trials. Ann Nutr Metab 55:173–201. https://doi.org/10.1159/000229002.
44. Forsythe CE, Phinney SD, Fernandez ML, Quann EE, Wood RJ, Bibus DM, Kraemer WJ, Feinman RD, Volek JS. 2008. Comparison of low fat and low carbohydrate diets on circulating fatty acid composition and markers of inflammation. Lipids 43:65–77. https://doi.org/10.1007/s11745-007-3132-7.
45. Volek JS, Phinney SD, Forsythe CE, Quann EE, Wood RJ, Puglisi MJ, Kraemer WJ, Bibus DM, Fernandez ML, Feinman RD. 2009. Carbohydrate restriction has a more favorable impact on the metabolic syndrome than a low fat diet. Lipids 44:297–309. https://doi.org/10.1007/s11745-008-3274-2.
46. Guilloteau P, Martin L, Eeckhaut V, Ducatelle R, Zabielski R, Van Immerseel F. 2010. From the gut to the peripheral tissues: the multiple effects of butyrate. Nutr Res Rev 23:366–384. https://doi.org/10.1017/S0954422410000247.
47. Van den Abbeele P, Grootaert C, Marzorati M, Possemiers S, Verstraete W, Gerard P, Rabot S, Bruneau A, El Aidy S, Derrien M, Zoetendal E, Kleerebezem M, Smidt H, Van de Wiele T. 2010. Microbial community development in a dynamic gut model is reproducible, colon region specific, and selective for Bacteroidetes and Clostridium cluster IX. Appl Environ Microbiol 76:5237–5246. https://doi.org/10.1128/AEM.00759-10.
48. Hill MJ. 1998. Composition and control of ileal contents. Eur J Cancer Prev 7(Suppl 2):S75–S78.
49. Cummings JH. 1978. Diet and transit through the gut. J Plant Foods 3:83–95. https://doi.org/10.1080/0142968X.1978.11904206.
50. Cummings JH, Jenkins DJ, Wiggins HS. 1976. Measurement of the mean transit time of dietary residue through the human gut. Gut 17:210–218. https://doi.org/10.1136/gut.17.3.210.
51. Macfarlane GT, Gibson GR, Cummings JH. 1992. Comparison of fermentation reactions in different regions of the human colon. J Appl Bacteriol 72:57–64. https://doi.org/10.1111/j.1365-2672.1992.tb04882.x.
52. Blazewicz SJ, Barnard RL, Daly RA, Firestone MK. 2013. Evaluating rRNA as an indicator of microbial activity in environmental communities: limitations and uses. ISME J 7:2061–2068. https://doi.org/10.1038/ismej.2013.102.
53. Muttray AF, Mohn WW. 1999. Quantitation of the population size and metabolic activity of a resin acid degrading bacterium in activated sludge using slot-blot hybridization to measure the rRNA:rDNA ratio. Microb Ecol 38:348–357. https://doi.org/10.1007/s002489901005.
54. Paliy O, Foy BD. 2011. Mathematical modeling of 16S ribosomal DNA amplification reveals optimal conditions for the interrogation of complex microbial communities with phylogenetic microarrays. Bioinformatics 27:2134–2140. https://doi.org/10.1093/bioinformatics/btr326.
55. Caporaso JG, Kuczynski J, Stombaugh J, Bittinger K, Bushman FD, Costello EK, Fierer N, Pena AG, Goodrich JK, Gordon JI, Huttley GA, Kelley ST, Knights D, Koenig JE, Ley RE, Lozupone CA, McDonald D, Muegge BD, Pirrung M, Reeder J, Sevinsky JR, Turnbaugh PJ, Walters WA, Widmann J, Yatsunenko T, Zaneveld J, Knight R. 2010. QIIME allows analysis of high-throughput community sequencing data. Nat Methods 7:335–336. https://doi.org/10.1038/nmeth.f.303.
56. Kembel SW, Wu M, Eisen JA, Green JL. 2012. Incorporating 16S gene copy number information improves estimates of microbial diversity and abundance. PLoS Comput Biol 8:e1002743. https://doi.org/10.1371/journal.pcbi.1002743.
57. Shankar V, Homer D, Rigsbee L, Khamis HJ, Michail S, Raymer M, Reo NV, Paliy O. 2015. The networks of human gut microbe-metabolite associations are different between health and irritable bowel syndrome. ISME J 9:1899–1903. https://doi.org/10.1038/ismej.2014.258.
58. David LA, Maurice CF, Carmody RN, Gootenberg DB, Button JE, Wolfe BE, Ling AV, Devlin AS, Varma Y, Fischbach MA, Biddinger SB, Dutton RJ, Turnbaugh PJ. 2014. Diet rapidly and reproducibly alters the human gut microbiome. Nature 505:559–563. https://doi.org/10.1038/nature12820.
59. O'Keefe SJ, Li JV, Lahti L, Ou J, Carbonero F, Mohammed K, Posma JM, Kinross J, Wahl E, Ruder E, Vipperla K, Naidoo V, Mtshali L, Tims S, Puylaert PG, DeLany J, Krasinskas A, Benefiel AC, Kaseb HO, Newton K, Nicholson JK, de Vos WM, Gaskins HR, Zoetendal EG. 2015. Fat, fibre and cancer risk in African Americans and rural Africans. Nat Commun 6:6342. https://doi.org/10.1038/ncomms7342.
60. Zhang C, Zhang M, Pang X, Zhao Y, Wang L, Zhao L. 2012. Structural resilience of the gut microbiota in adult mice under high-fat dietary perturbations. ISME J 6:1848–1857. https://doi.org/10.1038/ismej.2012.27.
61. Etxeberria U, Arias N, Boque N, Macarulla MT, Portillo MP, Milagro FI, Martinez JA. 2015. Shifts in microbiota species and fermentation products in a dietary model enriched in fat and sucrose. Benef Microbes 6:97–111. https://doi.org/10.3920/BM2013.0097.
62. Parks BW, Nam E, Org E, Kostem E, Norheim F, Hui ST, Pan C, Civelek M, Rau CD, Bennett BJ, Mehrabian M, Ursell LK, He A, Castellani LW, Zinker B, Kirby M, Drake TA, Drevon CA, Knight R, Gargalovic P, Kirchgessner T, Eskin E, Lusis AJ. 2014. Genetic control of obesity and gut microbiota composition in response to high-fat, high-sucrose diet in mice. Cell Metab 17:141–152. https://doi.org/10.1016/j.cmet.2012.12.007.
63. Perry RJ, Peng L, Barry NA, Cline GW, Zhang D, Cardone RL, Petersen KF, Kibbey RG, Goodman AL, Shulman GI. 2016. Acetate mediates a microbiome-brain-beta-cell axis to promote metabolic syndrome. Nature 534:213. https://doi.org/10.1038/nature18309.